Graph-Theoretic Analysis and Synthesis of Relative Sensing Networks

Daniel Zelazo and Mehran Mesbahi

Abstract—This work provides a general framework for the analysis and synthesis of a class of relative sensing networks (RSNs) in the context of its $\mathcal{H}_2$ and $\mathcal{H}_\infty$ performance. We consider RSNs with homogeneous and heterogeneous agent dynamics. In both cases, explicit graph theoretic expressions and bounds for the $\mathcal{H}_2$ and $\mathcal{H}_\infty$ performance are derived. The $\mathcal{H}_2$ performance turns out to be a function of the number of edges in the graph, whereas the $\mathcal{H}_\infty$ performance is structure dependent and related to the spectral radius of the graph Laplacian. The analysis results are then used to develop synthesis methods for RSNs. An optimal topology is designed using the Kruskal's Algorithm for $\mathcal{H}_2$ performance, and a semi-definite program for the $\mathcal{H}_\infty$ performance of uncertain RSNs.

Index Terms—Combinatorial optimization, graph theory, $\mathcal{H}_2$ and $\mathcal{H}_\infty$ performance, relative sensing networks, semi-definite programming.

I. INTRODUCTION

MULTI-AGENT systems pose significant challenges for control systems analysis and synthesis due to their inherently distributed sensing architectures. In particular, sensors must be associated with individual agents and their ability to measure state information from the entire ensemble—often in their local frames—can be limited by spatial constraints (such as orientation), range, and power requirements [35]. Fundamental questions such as how the sensing architecture affects the performance of the interconnected system and how control and estimation algorithms should be synthesized that exploit their distributed structure are the subjects of research across a wide range of disciplines.

In this work we focus on systems that rely on relative sensing to achieve their mission objectives; we call such systems *relative sensing networks* (RSNs). Relative sensing networks, in their most general form, are a collection of autonomous agents[1] that use sensed relative state information to achieve higher level objectives. In such systems, a *sensing topology* (or

graph) is induced by the spatial orientation of the agents and the capabilities of the relative sensor. In this way, the underlying sensing topology couples the agents at their outputs. Note that this type of model is in contrast to other multi-agent systems where the network coupling is introduced at the state level; see, for example, multi-agent consensus and synchronization problems [26], [31].

Relative sensing has become an important feature of many multi-agent systems. Space applications relying on relative sensing include spacecraft constellations for studying the structure of the heliopause, stereographic imaging and tomography for space physics, and space borne optical interferometry for probing the origins of the cosmos and identifying Earth-like planets [9], [12], [19], [25], [39]. Specifically, formation flying applications in deep space or GPS-denied environments must rely on relative sensing to achieve their objectives [8], [16], [28], [32], [33]. More fundamentally, these types of networks are relevant for applications involving distributed sensing for purposes of estimation and control with applications ranging from environmental surveillance, modeling, localization, and collaborative information processing [2], [4], [5], [22], [23], [30].

Fundamental to all these systems is the implicit presence of a "network." The exchange of information between each agent in an RSN describes an underlying connection topology. Studying system-theoretic notions from the perspective of the underlying topology can lead to interpretations that explicitly characterize the effects of the network on the behavior of the system. For linear time-invariant systems, all the essential systems theoretic properties can be derived from the quadruple system matrices (A, B, C, D). When considering multi-agent systems, the underlying connection topology, denoted as $\mathcal{G}$, can typically be embedded into the system matrices. It becomes enlightening to consider how certain properties of the system depend on that topology. Therefore, for linear multi-agent systems, one can consider the quintuple $(A, B, C, D, \mathcal{G})$ to emphasize the dependence of the overall system on its interconnections. Recent examples of such graph-centric analysis include relating closed-loop stability properties of multi-agent systems to the spectral properties of the graph Laplacian [11], relating controllability in consensus seeking systems to graph symmetry [29], [36], graph-theoretic analysis and performance bounds for consensus systems [7], [42], and graph-centric observability properties of relative sensing networks [37], [41].

The main contribution of this paper is a graph-centric characterization of the system $\mathcal{H}_2$ and $\mathcal{H}_\infty$ norms of RSNs for both analysis and synthesis purposes. A distinction is made between RSNs with homogeneous agent dynamics and RSNs with heterogeneous agent dynamics. Although homogeneous RSNs can

D. Zelazo is with the Institute for Systems Theory and Automatic Control, Universität Stuttgart, 70550 Stuttgart, Germany (e-mail: daniel.zelazo@ist.uni-stuttgart.de).

M. Mesbahi is with the Department of Aeronautics and Astronautics, University of Washington, Seattle, WA 98195-2400 USA (e-mail: mesbahi@uw.edu).

[1]An autonomous agent, depending on the application, may include unmanned vehicles, mobile sensors, or distributed computing nodes.

be considered as a subset of heterogeneous RSNs, it is more illuminating to consider these cases separately due to the algebraic simplicity of the former case.

For the synthesis portion of this paper we consider three general design scenarios. In the first, we examine how to design the connection topology to minimize the $\mathcal{H}_2$ and $\mathcal{H}_\infty$ norms of the overall RSN. This will point to an interesting connection between results in combinatorial optimization and systems theory. The second scenario is an inner-loop type control, where a local controller for each agent is designed such that its local performance is minimized in addition to a global performance metric focusing on the relative sensed output. Finally, we explore a decentralized outer-loop control using the sensed output as feedback to achieve higher order objectives, such as formation control.

The paper is organized as follows. Section I-A gives a brief overview of notions from algebraic graph theory and properties of the Kronecker product for matrices. In Section II, general models for homogeneous and heterogeneous RSNs are developed. Section III-A derives expressions for the $\mathcal{H}_2$ and $\mathcal{H}_\infty$ norms of homogeneous and heterogeneous RSNs, with an emphasis given to the role of the underlying topology. Section IV presents synthesis procedures for RSNs, and a few numerical examples are given in Section V.

A. Preliminaries and Notations

We provide some mathematical preliminaries and notations here. Matrices are denoted by capital letters (e.g., A), and vectors by lower case letters (e.g., x). Diagonal matrices will be written as $D = \mathbf{diag}\{d_1, \ldots, d_n\}$; this notation will also be employed for block-diagonal matrices and linear operators. A matrix and/or a vector that consists of all zero entries will be denoted by $\mathbf{0}$; whereas, '0' will simply denote the scalar zero. Similarly, the vector $\mathbf{1}$ denotes the vector of all ones, and $\mathbf{J} = \mathbf{1}\mathbf{1}^T$. The $n \times n$ identity matrix is denoted as I_n; we also append a subscript to $\mathbf{J}$, $\mathbf{1}$, and $\mathbf{0}$ to denote its dimension when it is not clear. The set of real numbers will be denoted as $\mathbb{R}$, and $\|.\|$ denotes the standard Euclidean 2-norm for vectors and matrices. For m-dimensional finite energy signals, that is signals in the space $\mathcal{L}_2^m$, the norm is induced by the inner-product and denoted as $\|u(j\omega)\|_{\mathcal{L}_2}^2 = \langle u(j\omega), u(j\omega) \rangle = \int_{-\infty}^{\infty} u(j\omega)^* u(j\omega) d\omega$. The $\mathcal{H}_2$ and $\mathcal{H}_\infty$ norms for linear operators will be denoted as $\|.\|_2$ and $\|.\|_\infty$. The adjoint of a linear operator f is denoted by f^*. The notation $A \circ B$ denotes the Hadamard product of the two matrices [20]. The Kronecker product of two matrices A and B is written as $A \otimes B$ [18].

An important result on Kronecker products relates the singular values of $A \otimes B$ to the matrices $A \in \mathbb{R}^{n \times m}$ and $B \in \mathbb{R}^{q \times r}$; $\sigma(A \otimes B) = \{\sigma_i(A)\sigma_j(B) i = 1, \ldots \min\{n, m\}, j = 1, \ldots, \min\{q, r\}\}$ [18]. An immediate consequence of this is the following result on the matrix 2-norm, $\|A \otimes B\| = \|A\|\|B\|$. We also make extensive use of the Kronecker product matrix multiplication property, $(A \otimes B)(C \otimes D) = (AC \otimes BD)$, where the matrices are all of commensurate dimensions.

Graphs and the matrices associated with them will be widely used in this work. The reader is referred to [14] for a detailed treatment of the subject. An undirected (simple) graph $\mathcal{G}$ is specified by a vertex set $\mathcal{V}$ and an edge set $\mathcal{E}$ whose elements characterize the incidence relation between distinct pairs of $\mathcal{V}$. Two
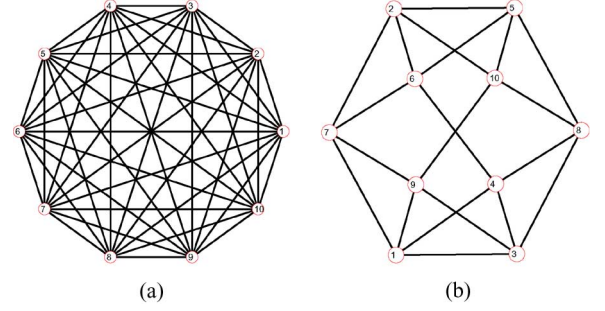

Fig. 1. Example of regular graphs. (a) K_{10} graph; (b) A 4-regular graph.

vertices i and j are called *adjacent* (or neighbors) when $\{i, j\} \in \mathcal{E}$; we denote this by writing $i \sim j$. An *orientation* of an undirected graph $\mathcal{G}$ is the assignment of directions to its edges, i.e., an edge e_k is an ordered pair (i, j) such that i and j are, respectively, the initial and the terminal nodes of e_k.

In this work we make extensive use of the $|\mathcal{V}| \times |\mathcal{E}|$ incidence matrix, $E(\mathcal{G})$, for a graph with arbitrary orientation. The incidence matrix is a $\{0, \pm 1\}$-matrix with rows and columns indexed by the vertices and edges of $\mathcal{G}$ such that $[E(\mathcal{G})]_{ik}$ has the value '+1' if node i is the initial node of edge e_k, '−1' if it is the terminal node, and '0' otherwise. The degree of vertex i, d_i, is the cardinality of the set of vertices adjacent to it. The degree matrix, $\Delta(\mathcal{G})$, and the adjacency matrix, $A(\mathcal{G})$, are defined in the usual way [14].

The (graph) Laplacian of $\mathcal{G}$

$$L(\mathcal{G}) := E(\mathcal{G})E(\mathcal{G})^T = \Delta(\mathcal{G}) - A(\mathcal{G}) \qquad (1.1)$$

is a rank deficient positive semi-definite matrix. The eigenvalues of the graph Laplacian are real and will be ordered and denoted as $0 = \lambda_1(\mathcal{G}) \leq \lambda_2(\mathcal{G}) \leq \cdots \leq \lambda_{|\mathcal{V}|}(\mathcal{G})$.

In order to apply the framework developed in this paper to specific graphs, we will work with the complete graph and its generalization in terms of k-regular graphs, which are defined as follows. The *complete graph* on n nodes, K_n, is the graph where all possible pairs of vertices are adjacent, or equivalently, if the degree of all vertices is $|\mathcal{V}| - 1$. Fig. 1(a) depicts K_{10}, the complete graph on 10 nodes. When every node in a graph with n nodes has the same degree $k \leq n - 1$, it is called a k-regular graph. Fig. 1(b) shows a 4-regular graph.

II. RELATIVE SENSING NETWORK MODEL

In this section we derive a general plant model for relative sensing networks. An RSN consists of two system layers. The first can be considered a local layer corresponding to the dynamics of the individual agents in the ensemble, whereas the global layer represents the coupling of each agent through the interconnection topology.

We identify two classes of RSNs in this paper: 1) homogeneous RSNs, and 2) heterogeneous RSNs. For both cases, we will work with a group of g dynamic systems (the "agents"), each modeled as a linear and time-invariant system

$$\Sigma_i : \begin{cases} \dot{x}_i(t) = A_i x_i(t) + B_i u_i(t) + \Gamma_i w_i(t) \\ z_i(t) = C_i^z x_i(t) + D_i^{zu} u_i(t) + D_i^{zw} w_i(t) \\ y_i(t) = C_i^y x_i(t) + D_i^{yw} w_i(t), \end{cases} \qquad (2.2)$$
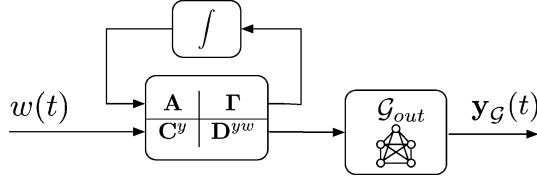
Fig. 2. Block diagram of global RSN Layer; the integrator feedback connection represents an upper fractional transformation [10].

where each agent is indexed by the sub-script i. Here, $x_i(t) \in \mathbb{R}^{n_i}$ represents the state, $u_i(t) \in \mathbb{R}^{m_i}$ the control, $w_i(t) \in \mathbb{R}^{r_i}$ an exogenous input,[2] $z_i(t) \in \mathbb{R}^{s_i}$ the controlled variable, and $y_i(t) \in \mathbb{R}^{q_i}$ the locally measured output.

We denote the transfer-function representation of Σ_i as $\hat{\Sigma}_i$

$$\hat{\Sigma}_i := \begin{bmatrix} C_i^z \\ C_i^y \end{bmatrix} (sI - A_i)^{-1} [B_i \quad \Gamma_i] + \begin{bmatrix} D_i^{zu} & D_i^{zw} \\ \mathbf{0} & D_i^{yw} \end{bmatrix}; \quad (2.3)$$

the transfer function for a particular input-output channel is denoted, for example, as $H_i^{yu} = C_i^y(sI - A_i)^{-1}B_i$.

In the homogeneous case, it is assumed that each dynamic agent in the RSN is described by the same set of linear state-space dynamics (e.g., $\Sigma_i = \Sigma_j$ for all i, j). When working with homogeneous RSNs, we drop the sub-script for all state-space and operator representations of the system. We will also assume no feed-forward terms of the control to the measured output. Additionally, we assume a minimal realization for each agent with compatible outputs for all agents, e.g., system outputs will correspond to the same physical quantity. It should be noted that in a heterogeneous system, the dimension of each agent need not be the same; however, using a "padding argument," it can be assumed that all agents have identical dimensions for their respective state space (e.g., $n_i = n_j = n$, for all i, j). We denote the map from $w_i(t)$ to $z_i(t)$ as $T_i^{w \mapsto z}$.

The parallel interconnection of all the agents can be expressed by a concatenation of the corresponding system states, inputs, and outputs, and through the block diagonal aggregation of each agent's state-space matrices. We use the bold-face notation to denote the expanded state-space, e.g., $\mathbf{x}(\mathbf{t}) = [x_1(t)^T, \ldots, x_g(t)^T]^T$ and $\mathbf{A} = \mathbf{diag}\{A_1, \ldots, A_g\}$.

The global RSN layer we examine in this paper is motivated by the relative sensing problem discussed in Section I. The sensed output of the RSN is the vector $\mathbf{y}_\mathcal{G}(t)$ containing relative state information of each agent and its neighbors. The incidence matrix of a graph naturally captures state differences and will be the algebraic construct used to define the relative outputs of RSNs. For example, the output sensed between agent i and agent j could be of the form $y_i(t) - y_j(t)$, and can be compactly written for the entire RSN as

$$\mathbf{y}_\mathcal{G}(t) = (E(\mathcal{G})^T \otimes I_q) \, \mathbf{y}(t). \quad (2.4)$$

Here, $\mathcal{G}$ is the graph the describes the connection topology of the RSN; the node set is given as $\mathcal{V} = \{1, \ldots, g\}$. The global layer is visualized in the block diagram shown in Fig. 2.

When considering the analysis of the global layer, we are interested in studying the map from the agent's exogenous inputs

to the RSN sensed output. Using the above notations we can express the heterogeneous RSN in a compact form

$$\Sigma_{het}(\mathcal{G}) \begin{cases} \dot{\mathbf{x}}(t) = \mathbf{A}\mathbf{x}(t) + \mathbf{B}\mathbf{u}(t) + \mathbf{\Gamma}\mathbf{w}(t) \\ \mathbf{z}(t) = \mathbf{C}^z\mathbf{x}(t) + \mathbf{D}^{zu}\mathbf{u}(t) + \mathbf{D}^{zw}\mathbf{w}(t) \\ \mathbf{y}(t) = \mathbf{C}^y\mathbf{x}(t) + \mathbf{D}^{yw}\mathbf{w}(t) \\ \mathbf{y}_\mathcal{G}(t) = (E(\mathcal{G})^T \otimes I) \, \mathbf{C}\mathbf{x}(t). \end{cases} \quad (2.5)$$

The homogeneous RSN, $\Sigma_{hom}(\mathcal{G})$, can be expressed using Kronecker products. For example, $\mathbf{A} = I_g \otimes A$ and $(E(\mathcal{G})^T \otimes I)\mathbf{C} = E(\mathcal{G})^T \otimes C$. Note that the local observation matrix for each agent, C_i^y, need not be the same as the observation matrix for the relative sensed measurement $\mathbf{y}_\mathcal{G}(t)$. For example, a relative position measurement would be of the form $(E(\mathcal{G})^T \otimes [I_3 \ 0])$, while the local measurement might contain additional information.

Similarly, the transfer function representation is denoted as $\hat{\Sigma}_{het}$ and is defined as in (2.3). As in the state space model, bold faced transfer functions denotes the block diagonal aggregation of each agent's corresponding transfer function, e.g., $\mathbf{H}^{zu}(s) = \mathbf{diag}\{H_1^{zu}(s), \ldots, H_g^{zu}(s)\}$. The homogeneous system, $\hat{\Sigma}_{hom}$, can also be written using the Kronecker product in a similar manner as described above.

For notational simplicity, we denote $T_{hom}^{w \mapsto \mathcal{G}}$ and $T_{het}^{w \mapsto \mathcal{G}}$ as the map from the exogenous inputs to the RSN sensed output for homogeneous and heterogeneous systems respectively, e.g., $T_{hom}^{w \mapsto \mathcal{G}} = E(\mathcal{G})^T \otimes H^{\mathcal{G}w}(s)$. We also use transfer function and state-space representations interchangeably noting the appropriate realization can be inferred by context. For example, H_i^{yw} will be used to represent both the state-space and transfer function representation of the open-loop map from the exogenous inputs to the measurement of agent i.

A. Observability Properties of RSNs

Examining the observability properties of RSNs can give both qualitative and quantitative insights about the utility of the sensed output for use in estimation and observer design. A natural question, therefore, is whether *the initial condition of each agent in an RSN can be inferred from their relative outputs* [41]. For such an analysis we work with a simplified version of (2.5)

$$\begin{cases} \dot{\mathbf{x}}(t) = \mathbf{A}\mathbf{x}(t) \\ \mathbf{y}_\mathcal{G}(t) = (E(\mathcal{G})^T \otimes I) \, \mathbf{C}\mathbf{x}(t). \end{cases} \quad (2.6)$$

Recall that the observability gramian of a linear system with state matrix A and observation matrix C is

$$Y_o = \int_0^\infty e^{A^T t} C^T C e^{At} dt. \quad (2.7)$$

The observability as well as the relative degree of observability of different modes in a linear system can be inferred from the gramian. For this analysis, we will assume that each agent is stable (e.g., A_i is Hurwitz) and that (A_i, C_i) is an observable pair.

1) Observability of Homogeneous RSNs: For homogeneous RSNs, the observability gramian can be immediately written as

$$\mathbf{Y}_o = L(\mathcal{G}) \otimes \int_0^\infty e^{A^T t} C^T C e^{At} dt = L(\mathcal{G}) \otimes Y_o \quad (2.8)$$

where Y_o is the gramian for an individual agent in the RSN. This expression has the following immediate consequence.

Theorem 2.1: The homogeneous RSN in (2.6) is unobservable.

Proof: Using (2.8) and the properties of the Kronecker product we conclude that $\mathbf{Y}_o$ has precisely n eigenvalues at the origin, leading to an unobservable system. ∎

The unobservable modes of (2.6) in fact, correspond to the "inertial state" of the formation; these modes lie in the subspace $\mathbf{span}\{\mathbf{1}_g \otimes I_n\}$. The importance of this observation is that when each agent has identical dynamics, relative measurements alone are not sufficient to reconstruct the inertial state of each agent. If in addition to the relative output, a measurement such as the inertial state of a single agent is available, then the observability of the system can be recovered.

This observation also highlights how the underlying connection topology can influence the relative degree of observability of the observable modes. Denote and index each singular values of Y_o as σ_i, and using the properties of the Kronecker product, we can express the non-zero singular values of $\mathbf{Y}_o$ as $\lambda_j(\mathcal{G})\sigma_i$ for $j = 2, \ldots, g$ and all i. The eigenvalues of the graph Laplacian, therefore, can amplify or attenuate the observability of certain modes in the system. For example, the complete graph shown in Fig. 1(a), has $\lambda_i(\mathcal{G}) = \lambda_j(\mathcal{G}) = g$ for all $i, j \geq 2$. In this case, the connection topology does not favor any particular mode of the system. Conversely, when the graph is disconnected with two connected components, then $\lambda_2(\mathcal{G}) = 0$ and n additional unobservable modes are introduced into the system.

2) Observability of Heterogeneous RSNs: In the heterogeneous case, the observability gramian of (2.6) has a non-trivial form. Let us define the observability operator for an individual agent as $\Psi_i(x) = C_i e^{A_i t}x$, and its adjoint as $\Psi_i^*(y(t)) = \int_0^\infty e^{A_i^T t}C_i^T y(t)dt$. The gramian of (2.6) can now be written as

$$\mathbf{Y}_o = \mathbf{diag}\{\boldsymbol{\Psi}^*\} \left(L(\mathcal{G}) \otimes I_n\right) \mathbf{diag}\{\boldsymbol{\Psi}\} = (L(\mathcal{G}) \otimes I_n) \circ \boldsymbol{\Psi}^* \boldsymbol{\Psi}$$

where $\boldsymbol{\Psi} = [\Psi_1 \ \cdots \ \Psi_g]$ [41].

Theorem 2.2: The heterogeneous RSN in (2.6) is unobservable if and only if the following conditions are met:

1) There exists an eigenvalue μ^* of $\mathbf{A}$ that is common to each A_i.
2) For all i, j, $A_i q_i = \mu^* q_i$ and $A_j q_j = \mu^* q_j$ would imply that $C_i q_i = C_j q_j$.

Proof: For the necessary condition, recall the pair (A, C) is unobservable if and only if there exists a non-zero vector q such that $Aq = \lambda q$ and $Cq = 0$, i.e., the Popov-Hautus-Belevitch test (PHB) [21]. For the system (2.6), the PHB test shows that unobservability implies conditions 1 and 2 above. For sufficiency, suppose that there exists a common eigenvalue μ^* for all A_i's. We can then construct an eigenvector for the matrix $\mathbf{A}$ as $q = [q_1^T, \ldots, q_g^T]^T$, with vectors q_i's for which $A_i q_i = \mu^* q_i$. By condition 2, we have that $\mathbf{C}q = \mathbf{1}_g \otimes r$, where $r = C_i q_i \neq 0$ for all i. Using properties of the Kronecker product we then have $(E(\mathcal{G})^T \otimes I)\mathbf{C}q = (E(\mathcal{G})^T \otimes I)(\mathbf{1}_g \otimes r) = (E(\mathcal{G})^T \mathbf{1}_g \otimes r) = 0$. This shows the system is unobservable with q as the corresponding unobservable mode. ∎

Theorem 2.2 reinforces that a heterogeneous RSN is unobservable only when the outputs of each agent associated with a certain initial direction becomes indistinguishable. This condition is rather strict, emphasizing that most real-world instances of a heterogeneous RSN is observable, allowing its inertial state to be reconstructed solely from the corresponding relative measurements.[3]

As in the homogeneous case, the underlying connection topology can have a profound affect on the relative degree of observability of the RSN. The form of (2.9) is appealing in how it separates the role of the network from the agents dynamics. Although the precise characterization of the eigen-values of (2.9) is non-trivial, bounds on those values can be derived, as presented in [20].

Corollary 2.3: The smallest and largest eigenvalues of the observability gramian (2.9) are bounded as

$$\underline{d}\,\underline{\sigma}(\boldsymbol{\Psi}^*\boldsymbol{\Psi}) \leq \underline{\sigma}(\mathbf{Y}_o) \leq \overline{\sigma}(\mathbf{Y}_o) \leq \overline{d}\,\overline{\sigma}(\boldsymbol{\Psi}^*\boldsymbol{\Psi}) \qquad (2.9)$$

where $\underline{\sigma}(\mathbf{Y}_o)$ and $\overline{\sigma}(\mathbf{Y}_o)$ correspond to, respectively, the smallest and largest singular values of $\mathbf{Y}_o$, and $\underline{d} = \min_i [L(\mathcal{G}) \otimes J_n]_{ii}$, $\overline{d} = \max_i [L(\mathcal{G}) \otimes J_n]_{ii}$; the quantities $\underline{d}$ and $\overline{d}$ correspond to the minimum and maximum degree vertices of the underlying graph.

This result points to an interesting connection between the degree of each agent in the ensemble and the relative observability of the modes of the system. This theme will be revisited when we study the $\mathcal{H}_2$ performance of heterogeneous RSNs. For a more in depth study on the observability of RSNs, the reader is referred to [41]. A similar analysis on the controllability of systems with input coupling is also presented in [43].

III. GRAPH THEORETIC BOUNDS ON RSN PERFORMANCE

In this section we explore a graph-theoretic characterization of the $\mathcal{H}_2$ and $\mathcal{H}_\infty$ performance of the RSN model presented in Section II. The main goal is to highlight the role of the underlying connection topology on the system norms mapping the exogenous inputs $\mathbf{w}(t)$ to the relative sensed output $\mathbf{y}_\mathcal{G}(t)$, $T^{w \mapsto \mathcal{G}}$. For both the $\mathcal{H}_2$ and $\mathcal{H}_\infty$ analysis, the homogeneous and heterogeneous cases are presented separately. We also assume that the observation matrix for the sensed output is the same as for the local measurement; that is $\mathbf{C} = \mathbf{C}^y$ and $\mathbf{H}^{\mathcal{G}w} = \mathbf{H}^{yw}$. Additionally, we assume throughout this section that the underlying connection graph $\mathcal{G}$ is connected and $\mathcal{V} = \{1, \ldots, g\}$. For analysis, we finally assume that each agent is stable; an assumption that will be relaxed in Section IV in the context of RSN synthesis.

A. $\mathcal{H}_2$ Performance

We first recall that one interpretation of the $\mathcal{H}_2$ performance of a linear system characterizes how a (Gaussian) exogenous noise propagates throughout the system and effects the energy of the monitored output. In the context of RSNs, therefore, *the $\mathcal{H}_2$ system norm can be employed to reason about how noise, corrupting each agent's dynamics in the network, results in the asymptotic deviation of the sensed output of the entire network.* This section aims to explicitly characterize the effect of the network structure on the $\mathcal{H}_2$ norm of the system.

---

[3]This assumes the linear dynamics of each agent are derived in the same coordinate frame.

The $\mathcal{H}_2$ norm of a system can be calculated in a variety of ways. One description involves the observability gramian of the system, as discussed in Section II-A. Another description involves the controllability gramian of the system. The controllability gramian for an individual agent (from the exogenous input channel) based on the dynamics in (2.2) is defined as

$$X_c^{(i)} = \int_0^\infty e^{A_i t} \Gamma_i \Gamma_i^T e^{A_i^T t} dt. \tag{3.10}$$

The $\mathcal{H}_2$ norm of each agent from the exogenous input channel to the measured output can be expressed in terms of the gramians as

$$\left\|H_i^{yw}\right\|_2^2 = \mathbf{tr}\left(\Gamma_i^T Y_o^{(i)} \Gamma_i\right) = \mathbf{tr}\left(C_i^y X_c^{(i)} (C_i^y)^T\right). \tag{3.11}$$

Using the above description we can begin to understand how the underlying network topology influences the system norm. Subsequently, we assume that $D_i^{zw} = 0$ and $D_i^{yw} = 0$ for our analysis, as the corresponding $\mathcal{H}_2$ norm of the network will otherwise be unbounded.

1) Homogeneous RSN $\mathcal{H}_2$ Performance: The $\mathcal{H}_2$ norm of the homogeneous RSN described in (2.5) can be derived using the observability gramian (2.8) to obtain the following result.

Theorem 3.1: The $\mathcal{H}_2$ norm of the homogeneous RSN (2.5) is given as

$$\left\|T_{hom}^{w\mapsto\mathcal{G}}\right\|_2 = \left\|E(\mathcal{G})\right\|_F \left\|H^{yw}\right\|_2. \tag{3.12}$$

Proof: The $\mathcal{H}_2$ norm can be written directly from (2.8) as $\left\|T_{hom}^{w\mapsto\mathcal{G}}\right\|_2^2 = \mathbf{tr}((I_g \otimes \Gamma)^T (L(\mathcal{G}) \otimes Y_o)(I_g \otimes \Gamma))$. Using the properties of the Kronecker product defined in Section I-A and the definition of the Frobenius norm of a matrix, $\|M\|_F^2 = \mathbf{tr}(M^T M) = \sum_{i=1}^n \|m_i\|_2^2$, leads to the expression in (3.12). Here, m_i represents the i-th column of $M \in \mathbb{R}^{n \times n}$. ∎

The expression in (3.12) gives an explicit characterization of how the network affects the overall gain of the RSN. In the homogeneous case, we can thereby focus on how the Frobenius norm of the incidence matrix changes with the addition or removal of an edge. Recall that each column of the incidence matrix represents an edge of the graph. Therefore, the Frobenius norm of the incidence matrix can be expressed in terms of the number of edges in the graph, $|\mathcal{E}|$, as $\|E(\mathcal{G})\|_F^2 = 2|\mathcal{E}|$. An immediate consequence of this description is that $\mathcal{H}_2$ norm of the RSN is only dependent on the number of edges in the network rather than its the actual structure.

If we consider only connected graphs, we arrive at the following corollary providing lower and upper bounds on the $\mathcal{H}_2$ norm of the system.

Corollary 3.2: The $\mathcal{H}_2$ norm of the homogeneous RSN (2.5) for an arbitrary connected graph $\mathcal{G}$ is bounded from below by an RSN where $\mathcal{G}$ is a spanning tree and bounded from above by an RSN where $\mathcal{G} = K_g$, the complete graph

$$2(g-1)\|H^{yw}\|_2^2 \leq \left\|T_{hom}^{w\mapsto\mathcal{G}}\right\|_2^2 \leq 2g(g-1)\|H^{yw}\|_2^2. \tag{3.13}$$

2) Heterogeneous RSN $\mathcal{H}_2$ Performances: For the heterogeneous case we rely on the identity (3.11) to derive the $\mathcal{H}_2$ norm. The connection topology only couples agents at the output

leading to a block diagonal description for the controllability gramian, with each block corresponding to (3.10).

Theorem 3.3: The $\mathcal{H}_2$ norm of the heterogeneous RSN (2.5) is given as

$$\left\|T_{het}^{w\mapsto\mathcal{G}}\right\|_2^2 = \sum_{i=1}^g d_i \left\|H_i^{yw}\right\|_2^2 = \left\|QE(\mathcal{G})\right\|_F^2 \tag{3.14}$$

where d_i is the degree of the i-th agent in the graph and $Q = \mathbf{diag}\{\|H_1^{yw}\|_2, \ldots, \|H_g^{yw}\|_2\}$.

Proof: The norm expression in (3.14) can be derived using (3.11) as, $\left\|T_{het}^{w\mapsto\mathcal{G}}\right\|_2^2 = \mathbf{tr}\{(E(\mathcal{G})^T \otimes I_q)\mathbf{C}^y\mathbf{X}_c(\mathbf{C}^y)^T(E(\mathcal{G}) \otimes I_q)\}$, where $\mathbf{X}_c$ denotes the block diagonal aggregation of each agent's controllability gramian, as defined in (3.10). In this direction, observe that $\mathbf{tr}\{\mathbf{C}^y\mathbf{X}_c(\mathbf{C}^y)^T\} = \sum_{i=1}^g \|H_i^{yw}\|_2^2$. Using the cyclic property of the trace operator [44] and exploiting the block diagonal structure of the matrix arguments leads to the desired result. ∎

When each agent has the same dynamics, (3.14) reduces to the expression in (3.12). This characterization paints a clear picture of how the placement of an agent within a certain topology affects the overall system gain. In order to minimize the network gain, it is beneficial to assign low connectivity to systems with large norm.

For certain graph structures, a more explicit characterization of the $\mathcal{H}_2$ performance can be derived, leading to the following corollaries.

Corollary 3.4: The $\mathcal{H}_2$ norm of the heterogeneous RSN (2.5) when the underlying connection graph is k-regular is

$$\left\|T_{het}^{w\mapsto\mathcal{G}}\right\|_2^2 = k \sum_{i=1}^g \|H_i^{yw}\|_2^2 \tag{3.15}$$

where every node has degree k.

Note that having regularity in the connection topology introduces 'homogeneity' into an otherwise heterogeneous RSN. As in the homogeneous case, the placement of an agent in such a network will not affect the overall performance; in fact, the system norm becomes a scaled version of the parallel connection of the g subsystems.

B. $\mathcal{H}_\infty$ Performance

We first recall that the $\mathcal{H}_\infty$ norm for a dynamic system captures how a measurable signal with finite energy, i.e., a signal in $\mathcal{L}_2$, is amplified at the monitored output of the system. Moreover, this norm has implications for robustness, disturbance rejection, and uncertainty management for dynamic systems. Specifically, the $\mathcal{H}_\infty$ norm of a linear system with transfer-function representation $H(s)$ is characterized as

$$\|H(j\omega)\|_\infty = \sup_\omega \{\overline{\sigma}[H(j\omega)]\} = \sup_{\|U\|_2=1} \|H(j\omega)U\|_{\mathcal{L}_2} \tag{3.16}$$

where $\overline{\sigma}[A]$ denotes the largest singular value of the matrix A. The induced-norm description allows us to state the sub-multiplicative property of the $\mathcal{H}_\infty$ norm for two operators as $\|H(j\omega)P(j\omega)\|_\infty \leq \|H(j\omega)\|_\infty\|P(j\omega)\|_\infty$.

In the context of RSNs, therefore, *the $\mathcal{H}_\infty$ system norm can be used to capture how disturbances and finite energy exogenous signals result in the asymptotic deviation of the sensed output*

of the network from the origin. This section aims to explicitly characterize the effect of the network on the $\mathcal{H}_\infty$ norm of the system. As in Section III-A, we separate our analysis into the homogeneous and heterogeneous cases.

1) Homogeneous RSN $\mathcal{H}_\infty$ Performance: Given the transfer function representation of the homogeneous RSN, we can write the map from the disturbances to the networked output as $\mathbf{Y}_\mathcal{G}(s) = (E(\mathcal{G})^T \otimes H^{yw})\mathbf{U}(s)$.

Theorem 3.5: The $\mathcal{H}_\infty$ norm of the homogeneous RSN (2.5) is given as

$$\left\| T_{hom}^{w \mapsto \mathcal{G}} \right\|_\infty = \|E(\mathcal{G})\| \, \|H^{yw}\|_\infty. \qquad (3.17)$$

Proof: The norm expression follows directly from the definition in (3.16) and the matrix 2-norm of Kronecker products.∎

The expression (3.17) states that the overall $\mathcal{L}_2$ gain of the system is proportional to the matrix 2-norm of the incidence matrix. In fact, since $\|E(\mathcal{G})\| = \sqrt{\|L(\mathcal{G})\|} = \lambda_g^{1/2}$, the behavior of the largest eigenvalue of the graph Laplacian is of particular interest. Moreover, an important observation is that certain graph structures will naturally lead to a smaller $\mathcal{H}_\infty$ norm. If we restrict our topology to spanning trees we can state a stronger set of results.

Corollary 3.6: When the underlying topology is a spanning tree, the path graph is the topology resulting in the smallest $\mathcal{H}_\infty$ norm for the homogeneous RSN (2.5). Moreover, the star graph is the topology resulting in the largest $\mathcal{H}_\infty$ norm for the homogeneous RSN (2.5).

Proof: In [34] it has been shown that the path graph has the smallest spectral norm for the graph Laplacian among all spanning trees. On the other hand, the star graph has the largest spectral norm for the graph Laplacian among all spanning trees [15]. These facts combined with the expression (3.17) conclude the proof.   ∎

Contrary to the results of Section III-A, we note that the structure of the graph plays a significant role in the $\mathcal{H}_\infty$ system performance as opposed to the $\mathcal{H}_2$ norm for homogeneous RSNs.

2) Bounds on the Heterogeneous RSN $\mathcal{H}_\infty$ Performance: We follow a similar procedure for the heterogeneous case. Using the transfer function representation of the heterogeneous RSN, we can write the map from the disturbances to the networked output as $\mathbf{Y}_\mathcal{G}(s) = (E(\mathcal{G})^T \otimes I_q)\mathbf{H}^{yw}(s)\mathbf{U}(s)$. Calculating the $\mathcal{H}_\infty$ norm involves finding the singular values of the transfer function

$$T_{het}^{w \mapsto \mathcal{G}} = \left(E(\mathcal{G})^T \otimes I_q \right) \mathbf{H}^{yw}(s). \qquad (3.18)$$

In general, an analytic expression for the singular values of the system in (3.18) is difficult to obtain. However, it is possible to derive bounds on the norm, leading to the following result.

Theorem 3.7: The $\mathcal{H}_\infty$ norm of the homogeneous RSN (2.5) is bounded as

$$\left\| T_{het}^{w \mapsto \mathcal{G}} \right\|_\infty \leq \|E(\mathcal{G})^T Q\| \leq \|E(\mathcal{G})^T\| \max_i \|H_i^{yw}\|_\infty \qquad (3.19)$$

where $Q = \mathbf{diag}\{\|H_1^{yw}\|_\infty, \ldots, \|H_g^{yw}\|_\infty\}$.

Proof: The upper-bound immediately arises from the sub-multiplicative property of the matrix 2-norm as $\|E(\mathcal{G})^T Q\| \leq \|E(\mathcal{G})^T\| \|Q\|$. Since Q is a diagonal matrix we conclude that

$\|Q\| = \max_i \|H_i^{yw}\|_\infty$. To show the lower-bound we follow the following chain of inequalities as

$$\left\| T_{het}^{w \mapsto \mathcal{G}} \right\|_\infty^2$$
$$= \sup_{\|U(j\omega)\|_{\mathcal{L}_2}=1} \left\| \left(E(\mathcal{G})^T \otimes I \right) \mathbf{H}^{yw}(j\omega)U(j\omega) \right\|_{\mathcal{L}_2}^2$$
$$= \sup_{\|U\|_{\mathcal{L}_2}=1} \int_{-\infty}^{\infty} U(j\omega)^* (\mathbf{H}^{yw})^* (L(\mathcal{G}) \otimes I) \mathbf{H}^{yw} U(j\omega) d\omega$$
$$= \sup_{\|U\|_{\mathcal{L}_2}=1} \int_{-\infty}^{\infty} \mathbf{tr}\left[U(j\omega)U(j\omega)^* (\mathbf{H}^{yw})^* \right.$$
$$\left. \times (L(\mathcal{G}) \otimes I) \mathbf{H}^{yw} \right] d\omega$$
$$\leq \sup_{\|U\|_{\mathcal{L}_2}=1} \int_{-\infty}^{\infty} \mathbf{tr}\left[U(j\omega)U(j\omega)^* \right]$$
$$\times \mathbf{tr}\left[(\mathbf{H}^{yw})^* (L(\mathcal{G}) \otimes I) \mathbf{H}^{yw} \right] d\omega$$
$$\leq \|QE(\mathcal{G})\| \qquad (3.20)$$

where the second to last inequality follows from the property that for Hermitian matrices, M and N, $\mathbf{tr}[MN] \leq \mathbf{tr}[M]\mathbf{tr}[N]$, and the last identity follows from the property that the positive-definite ordering $\mathbf{H}^{yw}(j\omega)^*(L(\mathcal{G}) \otimes I_q)\mathbf{H}^{yw}(j\omega) \leq (Q \otimes I_q)(L(\mathcal{G}) \otimes I_q)(Q \otimes I_q)$ holds for all ω.∎

Corollary 3.8: When each agent in (2.5) is a single-input single-output (SISO) system, the norm bound in (3.19) is tight.

An interesting implication of the norm bounds developed in the proof relates the $\mathcal{L}_2$ gain of a heterogeneous RSN to that of a homogeneous RSN. Consider an ordering of each agent in a heterogeneous RSN by the value of the $\mathcal{H}_\infty$ norm of each agent, $\|H_{k(1)}^{yw}\|_\infty \leq \cdots \leq \|H_{k(g)}^{yw}\|_\infty$, where $k : \{1, \ldots, g\} \mapsto \{1, \ldots, g\}$ maps the old index set to the norm-ordered one. The $\mathcal{H}_\infty$ norm of the heterogeneous system $T_{het}^{w \mapsto \mathcal{G}}$ can be bounded from above and below by homogeneous systems as

$$\|E(\mathcal{G})\| \left\| H_{k(1)}^{yw} \right\|_\infty \leq \left\| T_{het}^{w \mapsto \mathcal{G}} \right\|_\infty \leq \|E(\mathcal{G})\| \left\| H_{k(g)}^{yw} \right\|_\infty.$$

This inequality suggests that in addition to the structure of the underlying topology, one can consider the dynamic differences between agents as an important factor in the performance of the overall system.

IV. SYNTHESIS OF RELATIVE SENSING NETWORKS

In this section we explore various scenarios for the synthesis of RSNs using the results of Section III to motivate appropriate graph-centric objective functions. We consider three general type of synthesis problems: (1) Topology design, (2) Inner-loop control design for each agent, (3) Decentralized outer-loop control design. In each design scenario, we are primarily concerned with minimizing the performance objective $\|T_{het}^{w \mapsto \mathcal{G}}\|_p$; each objective function will contain an element related to the sensed output $y_\mathcal{G}(t)$. We will assume for the remainder of this section that the relative output of the RSN corresponds to a relative 'position' measurement between each agent as

$$\mathbf{y}_\mathcal{G}(t) := E(\mathcal{G})^T \otimes [I_c \quad 0] = E(\mathcal{G})^T \otimes C_c; \qquad (4.21)$$

here we have assumed the states corresponding to the position of each agent are the first c states of $x_i(t)$.

A. Topology Design

We now consider the synthesis of the underlying connection topology and where to place agents within that topology. As we are only considering the topology, we use the following heterogeneous state-space model for the RSN

$$T_{het}^{w\mapsto\mathcal{G}} : \begin{cases} \dot{\mathbf{x}}(t) = \mathbf{A}\mathbf{x}(t) + \mathbf{\Gamma}\mathbf{w}(t) \\ \mathbf{y}_{\mathcal{G}}(t) = \left(E(\mathcal{G})^T \otimes C_c\right)\mathbf{x}(t). \end{cases} \quad (4.22)$$

We would like to find topologies that minimize the effect of disturbances entering each agent on the relative sensed output of the entire system, that is minimizing the performance objective $\|T_{het}^{w\mapsto\mathcal{G}}\|_p$. This can be considered a problem in combinatorial optimization [24], as the decision to include an edge in the graph is binary. The general synthesis problem can be written as

$$\min_{\mathcal{G}} \left\|T_{het}^{w\mapsto\mathcal{G}}\right\|_p \quad \text{such that } \mathcal{G} \text{ is connected.}$$

The challenge, therefore, is to find numerically tractable algorithms to solve (4.23). In what follows, we show that the topology synthesis problem can be solved using the celebrated Kruskal's algorithm for finding a minimum weight spanning tree when $p = 2$. For $p = \infty$, we solve a variation of (4.23) that minimizes the robust performance of a weighted version of (4.22) with uncertainty on the edge weights.

1) $\mathcal{H}_2$ Topology Design: Recall from Section III-A that in terms of the $\mathcal{H}_2$ norm objective, an optimal topology should always correspond to a spanning tree. The design problem, therefore, is to determine which spanning tree will achieve the smallest $\mathcal{H}_2$ norm for the RSN (4.22).

The design of the topology reduces to the design of the incidence matrix, $E(\mathcal{G})$. This problem is combinatorial in nature, as there are only a finite number of graphs that can be constructed from a set of g nodes. As the number of agents in the RSN becomes large, solving this problem becomes prohibitively hard [24]. However, we find that with an appropriate modification of the problem statement, results from combinatorial optimization can be used, leading to a polynomial-time algorithm.

Specifically, the *minimum spanning tree* (MST) problem can be adapted to solve (4.23). The MST can be efficiently solved using Kruskal's algorithm in $\mathcal{O}(|\mathcal{E}|\log(|\mathcal{V}|))$ time. The procedure is given in **Algorithm 1** and a proof of its correctness can be found, for example, in [24].

Algorithm 1: Kruskal's Algorithm

Data: A connected undirected graph $\mathcal{G}(\mathcal{V},\mathcal{E})$ and weights $w : \mathcal{E} \mapsto \mathbb{R}$.

Result: A spanning tree $\mathcal{G}_t$ of minimum weight.

begin

    Sort the edges such that

    $w(e_1) \le w(e_2) \le \cdots \le w(e_{|\mathcal{E}|})$, where $e_i \in \mathcal{E}$

    Set $\mathcal{G}_t := \mathcal{G}_t(\mathcal{V}, \emptyset)$

    for $i := 1$ **to** $|\mathcal{E}|$ **do**

        if $\mathcal{G}_t + e_i$ *contains no cycle* **then**

            set $\mathcal{G}_t := \mathcal{G}_t + e_i$

In order to apply the MST to the $\mathcal{H}_2$ synthesis problem we must reformulate the original problem statement. To begin, we first write the expression for the $\mathcal{H}_2$ norm of the system in (4.22) as $\|T_{het}^{w\mapsto\mathcal{G}}\|_2^2 = \sum_{i=1}^g d_i \mathbf{tr}\{C_c X_i C_c^T\} = \sum_{i=1}^g d_i \|T_i^{w\mapsto c}\|_2^2$, where $T_i^{w\mapsto c}$ is the map from the exogenous input entering agent i to its position, $C_c x_i(t)$. We reiterate here that the RSN norm description is related to the degree of each node in the network. Using the weighted incidence graph interpretation of the norm, as in (3.14), we see that the gain of each agent, $\|T_i^{w\mapsto c}\|_2^2$, acts as a weight on the nodes.

As each agent is assumed to have fixed dynamics, the problem of minimizing the RSN $\mathcal{H}_2$ norm reduces to finding the degree of each agent while ensuring that the resulting topology is a spanning tree. This objective is related to properties of the nodes of the graph. To use the MST results, we must convert the objective from weights on the nodes to weights on the edges.

To develop this transformation, consider the graph $\mathcal{G} = (\mathcal{V}, \mathcal{E})$ with fixed weights f_i on each node ($i = 1, \ldots, g$). The node-weighted Frobenius norm of the incidence matrix is then $\|QE(\mathcal{G})\|_F^2 = \sum_i d_i f_i^2$, where $Q = \mathbf{diag}(f_1, \ldots, f_g)$. Next, consider the effect of adding an edge $\hat{e} = (i, j)$ to $\mathcal{E}$ in terms of the Frobenius norm of the augmented incidence matrix, $\|Q[E(\mathcal{G}) \; \hat{e}]\|_F^2 = \left(\sum_k d_k f_k^2\right) + f_i^2 + f_j^2$, where d_k represents the degree of node k *before* adding the new edge $\hat{e}$. This shows that each edge $\hat{e} = (i, j)$ contributes $(f_i^2 + f_j^2)$ to the overall norm. Therefore, weights on the edges, which we denote as $\mathbf{f}_e \in \mathbb{R}^{|\mathcal{E}| \times |\mathcal{E}|}$, can be constructed by adding the node weights, denoted as $\mathbf{f}_n = [f_1 \; \cdots \; f_g]^T$, corresponding to the nodes adjacent to each edge as, $\mathbf{f}_e = |E(\mathcal{G})^T|\mathbf{f}_n^2$.

This result can be used to generate an equivalent characterization of the $\mathcal{H}_2$-norm

$$\left\|T_{het}^{w\mapsto\mathcal{G}}\right\|_2^2 = \left\|\left[\|T_1^{w\mapsto c}\|_2^2 \quad \cdots \quad \|T_g^{w\mapsto c}\|_2^2\right]|E(\mathcal{G})|\right\|_1 \quad (4.23)$$

where $\|x\|_1 = \sum_i |x_i|$.

Using the above transformation from node weights to edge weights, we arrive at the following result.

Theorem 4.1: The connection topology that minimizes the $\mathcal{H}_2$ norm of (4.22), can be found using Kruskal's MST algorithm with input data $\mathcal{G}$, and edge weights $w = \left([\|T_1^{w\mapsto c}\|_2^2 \; \cdots \; \|T_g^{w\mapsto c}\|_2^2]|E(\mathcal{G})|\right)^T$.

Proof: The proof follows from Theorem 3.3 and the transformation from node weights to edge weights. ∎

Remark 4.2: The choice of the input graph $\mathcal{G}$ may be application specific, and can capture certain communication or sensing constraints between agents. For example, one may consider a scenario where agents are randomly distributed, e.g., as a geometric random graph, upon deployment and can then only sense neighboring agents within a specified range. The results of Theorem 4.1 can be used to determine the optimal spanning tree for that initial configuration.

Remark 4.3: There are a number of distributed algorithms for solving the MST problem [3], [13]. These could be used in place of the centralized version when the optimal spanning tree topology needs to be reconfigured. This scenario can arise due to the initialization problem discussed in Remark 4.2, or in situations when certain agents are disabled, lost, or reallocated for different mission purposes.

If there are no initial constraints on the input graph for Theorem 4.1, then we arrive at the following result.

Corollary 4.4: When the input graph in Theorem 4.1 is the complete graph, then the star graph with center node corresponding to the agent with minimum norm is the (non-unique) optimal topology.

Proof: The degree of the center node in a star graph is $g - 1$, and all other nodes have degree one. Assuming the node weights are sorted as $f_1 \leq \cdots \leq f_g$, then the $\mathcal{H}_2$ norm of the RSN is $\|T_{het}^{w \mapsto \mathcal{G}}\|_2^2 = (g - 1)f_1 + \sum_{i=2}^g f_i$. Any other tree can be obtained by removing and adding a single edge, while ensuring connectivity. With each such operation, the cost is nondecreasing, as any new edge will increase the degree of node $i > 1$ and by assumption $f_1 \leq f_i$. ∎

Corollary 4.4 shows that if there are no restrictions on the initial configuration, the optimal topology can be obtained without the MST algorithm. The computational effort required is only to determine the agent with smallest norm. The non-uniqueness of the star graph can occur if certain agents have identical norms, resulting in other possible configuration with an equivalent overall cost.

2) $\mathcal{H}_\infty$ Topology Design: Motivated by the results of Section III-B, we find that (4.23) reduces to the minimization of the spectral norm of the weighted incidence matrix, $\|QE(\mathcal{G})\|$, where Q was defined in Theorem 3.7. Minimization of this objective can be formulated as a mixed-integer semi-definite program. For reasonably sized problem instances this can be solved using, for example, branch-and-bound algorithms [24].

While topology design is an important application, the $\mathcal{H}_\infty$ framework allows us to consider the robustness of certain topologies. In this direction, we consider a variation of (4.23) that aims to minimize the *robust performance* of the RSN in (4.22). For such an analysis, we adjust the RSN model to allow for uncertainty in the sensing protocol. Specifically, we introduce the notion of a weighted edge for the sensed output. This model might be used to capture the fidelity of a relative measurement

$$T_{het}^{w \mapsto \mathcal{G}}(W_o) : \begin{cases} \dot{\mathbf{x}}(t) = \mathbf{A}\mathbf{x}(t) + \bar{\mathbf{\Gamma}}\mathbf{w}(t) \\ \mathbf{y}_\mathcal{G}(t) = \left(W_o E(\mathcal{G})^T \otimes C_c\right)\mathbf{x}(t). \end{cases} \quad (4.24)$$

In (4.24), each diagonal entry of $W_o = \mathbf{diag}\{w_1, \ldots, w_{|\mathcal{E}|}\}$ represents the nominal weights on each edge in the graph. A weight of zero corresponds to the absence of an edge. We will also assume all the weights are non-negative. The model (4.24) relates to (4.22) through the output as $T_{het}^{w \mapsto \mathcal{G}}(W_o) = (W_o \otimes I_c)T_{het}^{w \mapsto \mathcal{G}}$.

Using (4.24), we can introduce a structured uncertainty on each edge weight. The uncertainty set is defined as

$$\mathbf{\Delta}_w = \left\{\mathrm{diag}\left\{\delta_1, \ldots, \delta_{|\mathcal{E}|}\right\} : \delta_i \in \mathbb{R}, |\delta_i| \leq 1\right\}. \quad (4.25)$$

The true edge weight can thus be written as $W = W_o + \Delta$, for $\Delta \in \mathbf{\Delta}_w$. This can be considered as an output-multiplicative uncertainty, as shown in Fig. 3.

The problem (4.23) can now be restated as the *robust optimization* problem [6]

$$\min_{W_o} \max_{\|\mathbf{\Delta}\| \leq 1} \|QE(\mathcal{G})(W_o + \mathbf{\Delta})\| \text{ s.t. } \mathcal{G} \text{ is connected.} \quad (4.26)$$

This problem can be solved as a semi-definite program, the procedure of which is outlined in [6]. To apply these results, we
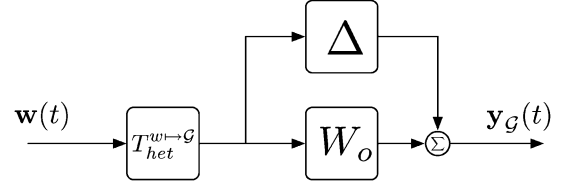

Fig. 3. Multiplicative uncertainty for NDS.

must express the objective and constraints of (4.26) as a perturbed LMI in the form

$$F(x, \delta) = F_0(x) + \sum_{i=1}^l \delta_i F_i(x) \quad (4.27)$$

where each $F_i(x)$ is a symmetric matrix and affine in the variable x.

First, we scalarize the objective function by introducing a new variable γ and noting that $\|QE(\mathcal{G})(W_o + \mathbf{\Delta})\| \leq \gamma$ can be written (via the Schur complement) as the LMI

$$\begin{bmatrix} \gamma I_g & QE(\mathcal{G})(W_o + \mathbf{\Delta}) \\ (W_o + \mathbf{\Delta})E(\mathcal{G})^T Q & I_{|\mathcal{E}|} \end{bmatrix} \geq 0. \quad (4.28)$$

Defining the matrices $S_i \in \mathbb{R}^{|\mathcal{E}| \times |\mathcal{E}|}$ and $V(\gamma)$ as

$$[S_i]_{kl} = \begin{cases} 1 & k = l = i \\ 0 & \text{otherwise,} \end{cases} \quad V(\gamma) = \begin{bmatrix} \gamma I_g & \mathbf{0} \\ \mathbf{0} & I_{|\mathcal{E}|} \end{bmatrix} \quad (4.29)$$

we can express (4.28) in the form (4.27) as

$$F_1(w, \delta) = V(\gamma) + \sum_{i=1}^{|\mathcal{E}|} (w_i + \delta_i) \begin{bmatrix} \mathbf{0}_g & QE(\mathcal{G})S_i \\ S_i E(\mathcal{G})^T Q & \mathbf{0}_{|\mathcal{E}|} \end{bmatrix}. \quad (4.30)$$

Similarly, the robust connectivity constraint can also be expressed in the form (4.27). Recall that for a connected graph, $\lambda_2(\mathcal{G}) > 0$, and the eigenvector associated with $\lambda_1(\mathcal{G}) = 0$ is the vector of all ones, $\mathbf{1}_g$. Defining the matrix P such that $\mathbf{IM}\{P\} = \mathbf{span}\{\mathbf{1}_g^\perp\}$, we obtain

$$F_2(w, \delta) = \sum_{i=1}^{|\mathcal{E}|} (w_i + \delta_i) P^T \left(e_i e_i^T\right) P > 0. \quad (4.31)$$

Using (4.30) and (4.31) we define $F_0^2(w) = P^T E W_o E^T P$, $F_i^2 = P^T e_i e_i^T P$, and[4]

$$F_0^1(w) = \begin{bmatrix} \gamma I_g & QEW_o \\ W_o E^T Q & I_{|\mathcal{E}|} \end{bmatrix}, \quad F_i^1 = \begin{bmatrix} \mathbf{0}_g & QES_i \\ S_i E^T Q & \mathbf{0}_{|\mathcal{E}|} \end{bmatrix}. \quad (4.32)$$

The above expressions can now be applied to the results in [6] to obtain the following SDP:

$$\begin{aligned} \min_{w, S_i, T_i} \quad & \gamma \\ \text{s.t.} \quad & \begin{bmatrix} S_i & F_1^i & \cdots & F_{|\mathcal{E}|}^i \\ F_1^i & T_i & & \\ \vdots & & \ddots & \\ F_{|\mathcal{E}|}^i & & & T_i \end{bmatrix} \geq 0, \quad i = 1, 2 \\ & S_i + T_i \leq 2F_0^i, \quad i = 1, 2, \\ & \sum_i w_i = \alpha, \quad w_i \in [0, w_{max}]. \end{aligned} \quad (4.33)$$

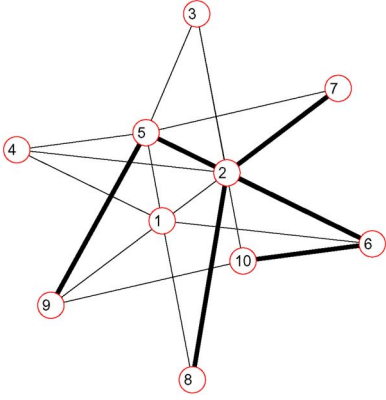[4] Here we streamline our notation as $E = E(\mathcal{G})$

Fig. 4. Optimal weighted topology; only edges with $w_i > 0.1$ are drawn in the corresponding weighted complete graph.

Fig. 5. Inner-loop design; the feedback connection represents an upper fractional transformation [10].

where the last two constraints, respectively, constrain the aggregate edge weight sum and the edge weight range.

To illustrate this procedure, we consider an RSN with $g = 10$ heterogeneous SISO systems (generated randomly in MATLAB). The input graph is the complete graph, K_g, allowing the program in (4.33) to select the optimal weights on every possible edge combination. For $\alpha = g-1$ and $w_{max} = 2$, (4.33) was solved using SeDuMi and YALMIP [27] in Matlab. The resulting weighted topology is shown in Fig. 4. Note that every edge has a positive weight (a complete weighted graph), however, only edges with $w_i > 0.1$ were drawn. The thickness of the line indicates a larger weight.

Remark 4.5: The formulation of the robust topology design does not include any constraints enforcing sparsity for the graph. The thresholding of edge weights discussed above is for visualization purposes. Indeed, thresholding the edge weights to generate sparse graphs can be done only with a loss of guarantees on connectedness and performance.

Remark 4.6: The above problem formulation can be extended to include dynamic edge weights. For example, each relative sensor may be characterized by a frequency dependent weight, $w_i(s)$, and the corresponding uncertainty can be considered as an unstructured norm-bounded uncertainty.

Remark 4.7: It should be noted that due to the auxiliary variables defined in (4.33), the size of this problem can grow large with the number of nodes. While interior-point methods offer polynomial-time algorithms, for excessively large problem instances, solving the corresponding SDP (4.33) might lead to numerical issues.

B. Inner-Loop Controller Design

We now consider the problem of designing a local control for each agent such that both local performance objectives are achieved in addition to the global RSN objective, $\|T_{het}^{w\mapsto\mathcal{G}}\|_p$, as shown in Fig. 5. In this scenario, the connection topology is given and fixed. From a synthesis point of view, each agent behaves independently and does not use information from the RSN for its control; this can be considered an inner-loop type of control design. Therefore, the general synthesis problem has the form

$$\min_{K_i} \left\|T_{het}^{w\mapsto\mathcal{G}}\right\|_p + \sum_i \left\|T_i^{w\mapsto z}\right\|_p \text{ s.t. } T_i^{w\mapsto z} \text{ stable,}$$

$$i = 1, \ldots, g.$$
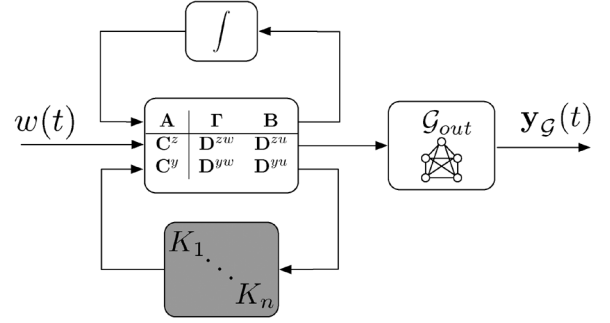
We note that while $\|T_i^{w\mapsto z}\|_p$ represents a purely local objective for each agent, the term $\|T_{het}^{w\mapsto\mathcal{G}}\|_p$ introduces a coupling between all the agents.

For $p = 2$, we present a semi-definite program that solves (4.34) with the additional feature of having a decentralized structure.

1) $\mathcal{H}_2$ Inner-Loop Design: For the duration of this section, we will assume that each agent has full-state feedback available for its control ($C_i^y = I$). The model we consider is (2.5), with $\mathbf{y}_\mathcal{G}(t)$ defined in (4.21). Note that $\mathbf{y}_\mathcal{G}(t)$ will be treated as an additional controlled variable for the $\mathcal{H}_2$ synthesis problem.

The state-feedback optimal $\mathcal{H}_2$ control problem for a single agent, without considering the global RSN objective, can be formulated as an SDP; see for example [10]. The global RSN performance objective can be appended to the standard SDP formulation for the $\mathcal{H}_2$ control of all agents connected in parallel, thus introducing a coupling constraint between each agents. The modified SDP formulation leads to the following result.

Theorem 4.8: Given the RSN system described in (2.5), a local state-feedback controller of the form $u_i(t) = K_i x_i(t)$ that minimizes local performance objectives in addition to the global RSN performance objective can be found by solving

$$\min_{W_i, X_i, Z_i, V_i} \quad \sum_{i=1}^{g} \mathbf{tr}[W_i] + \mathbf{tr}[V_i] \qquad (4.34)$$

$$\text{s.t.} \quad [A_i \; B_i]\begin{bmatrix} X_i \\ Z_i \end{bmatrix} + [X_i \; Z_i^T]\begin{bmatrix} A_i^T \\ B_i^T \end{bmatrix} + \Gamma_i\Gamma_i^T \leq 0 \quad (4.35)$$

$$\begin{bmatrix} X_i & (C_i^z X_i + D_i^{zu} Z_i)^T \\ (C_i^z X_i + D_i^{zu} Z_i) & W_i \end{bmatrix} > 0 \quad (4.36)$$

$$\begin{bmatrix} X_i & (C_p X_i)^T \\ C_p X_i & \frac{1}{d_i} V_i \end{bmatrix} > 0 \qquad (4.37)$$

with $K_i = Z_i X_i^{-1}$.

Proof: Consider the control $\mathbf{u}(t) = \mathbf{K}\mathbf{x}(t)$ implemented, where $\mathbf{K} = \mathbf{diag}(K_1, \ldots, K_n)$. The closed-loop system becomes

$$\Sigma_{cl}\begin{cases} \dot{\mathbf{x}}(t) = (\mathbf{A} + \mathbf{BK})\mathbf{x}(t) + \mathbf{\Gamma}\mathbf{w}(t) \\ \begin{bmatrix} \mathbf{z}(t) \\ \mathbf{y}_\mathcal{G}(t) \end{bmatrix} = \begin{bmatrix} \mathbf{C}^z + \mathbf{D}^{zu}\mathbf{K} \\ E(\mathcal{G})^T \otimes C_c \end{bmatrix}\mathbf{x}(t). \end{cases} \quad (4.38)$$

To guarantee the stability of the closed loop system, we require that $(\mathbf{A} + \mathbf{BK})$ be Hurwitz. This is guaranteed by the LMI given in (4.35) by noting the block diagonal structure of the matrix, and defining $Z_i = K_i X_i$. In fact, we note that X_i is

the generalized controllability gramian for the system in (4.38). In the meantime, the $\mathcal{H}_2$ norm of (4.38) can be calculated as

$$
\begin{aligned}
\|\Sigma_{cl}\|_2^2 &= \mathbf{tr}\left\{ \begin{bmatrix} \mathbf{C}^z + \mathbf{D}^{zu}\mathbf{K} \\ E(\mathcal{G})^T \otimes C_c \end{bmatrix} \mathbf{X} \begin{bmatrix} \mathbf{C}^z + \mathbf{D}^{zu}\mathbf{K} \\ E(\mathcal{G})^T \otimes C_c \end{bmatrix}^T \right\} \\
&= \mathbf{tr}\left\{ (\mathbf{C}^z + \mathbf{D}^{zu}\mathbf{K})\mathbf{X}(\mathbf{C}^z + \mathbf{D}^{zu}\mathbf{K})^T \right\} \\
&\quad + \mathbf{tr}\left\{ \left(E(\mathcal{G})^T \otimes C_c \right)\mathbf{X}\left(E(\mathcal{G})^T \otimes C_c \right)^T \right\} \quad (4.39)
\end{aligned}
$$

where $\mathbf{X} = \mathbf{diag}(X_1, \ldots, X_g)$. The first term on the right-hand side corresponds precisely to the $\mathcal{H}_2$ norm of the parallel interconnection of all agents when the feedback law $\mathbf{u}(t) = \mathbf{K}\mathbf{x}(t)$ implemented. The second term is the $\mathcal{H}_2$ norm of $T_{het}^{w\mapsto\mathcal{G}}$. Using the results from Section III-A we can thereby express the performance as $\|T_{het}^{w\mapsto\mathcal{G}}\|_2^2 = \sum_{i=1}^{g} d_i \mathbf{tr}\{C_c X_i C_c^T\}$.

The objective is to minimize $\|\Sigma_{cl}\|_2$, which can be accomplished by minimizing both terms in the right-hand side of (4.39). Using the matrix Schur-complement [18], we note that

$$
d_i C_c X_i C_c^T < V_i \text{ is equivalent to } \begin{bmatrix} X_i & (C_c X_i)^T \\ C_c X_i & \frac{1}{d_i} V_i \end{bmatrix} > 0.
$$

We now note that if $d_i C_c X_i C_c^T < V_i$, then $d_i \mathbf{tr}\{C_c X_i C_c^T\} < \mathbf{tr}\{V_i\}$. A similar derivation is used to arrive at the LMI in (4.36). ∎

Remark 4.9: The full-state feedback assumption can be relaxed without loss of generality using an LMI formulation for the more general output-feedback problem (such as LQG) [38]. The LMI (4.36) will consequently be modified, but the LMI corresponding to the global RSN performance (4.37) remains the same.

A striking feature of the SDP (4.34)–(4.37) is its structure. Although the global RSN layer couples each agent, we see that the coupling can be removed via the formulation of the $\mathcal{H}_2$ norm. The SDP is therefore 'separable' across each of the agents which has implications for the parallelization of the computation and decision-making process.

C. Outer-Loop Controller Design

In this section we consider the scenario where the sensed output $\mathbf{y}_\mathcal{G}(t)$ is used for feedback to each agent's control. This can be likened to an outer-loop control design where the RSN output may be used to achieve higher level objectives such as formation control. A desirable feature for this problem is to design a decentralized controller, i.e., the controller $K(\mathcal{G})$ should only use measurements local to each agent as determined by the connection topology $\mathcal{G}$.

A natural choice for a decentralized controller is one that inherits the underlying connection topology of the graph. Just as the incidence matrix captures the action of a relative position sensor, it can also be used as a means to distribute information to each node. A well studied model that employs such a protocol is the consensus protocol and its generalization [26], [31], [42]. In consensus type problems, each agent, via local interactions, reach agreement on a particular value of interest (e.g., a heading angle for a team of UAVs). Consider a collection of g agents each with first-order integrator dynamics corrupted with process noise as

$$
\dot{x}_i(t) = u_i(t) + w_i(t); \quad i = 1, \ldots, g. \quad (4.40)
$$

The objective of the team is for each agent to reach a common value for their state. This objective is naturally captured by the relative state information, and when the connection topology is given the controlled variable can be written as $z(t) = E(\mathcal{G})^T x(t)$.

When the performance variable is also available for feedback, a natural choice for a decentralized controller utilizes the underlying connection topology, such as $u(t) = -E(\mathcal{G})x(t)$. This, in turn, results in the closed-loop system

$$
\Sigma : \begin{cases} \dot{x}(t) = -L(\mathcal{G})x(t) + w(t) \\ z(t) = E(\mathcal{G})^T x(t). \end{cases} \quad (4.41)
$$

While the rate of convergence of (4.41) is one of the most studied aspect of consensus problems, it becomes immediately apparent that when cast as an RSN, allows for richer notions of performance to be examined. When the connection topology is permitted to be designed, the framework presented here allows to consider both the traditional aspects of consensus (e.g., rate of convergence) along with additional notions of performance, such as $\mathcal{H}_2$ or $\mathcal{H}_\infty$. The implications of this type of analysis in consensus problems have been explored in [42].

V. AN EXAMPLE

In this section we consider an application of our results to a mission scenario related to the *Autonomous NanoTechnology Swarm* project, or ANTS, currently under investigation by NASA [1]. One component of the ANTS mission involves the deployment of 1,000 pico-satellites to the asteroid belt for observational study. En-route to the asteroid belt the spacecraft must organize into smaller teams that will coordinate to search for various resources and materials.

For the formation of teams, a scenario might be to consider a formation topology that minimizes the $\mathcal{H}_2$ performance of the team, corresponding to the results developed in Section IV-A-1. For this example, we will consider a system comprised of 75 heterogeneous pico-satellites. Each agent's state-space was generated randomly using MATLAB, with a single input and a single output (corresponding to the position variable, as in C_c defined in (4.21)). The agents are randomly distributed and the initial topology is determined by assigning an edge between two agents if their Euclidean distance is less than $r = 0.20$. This could correspond to the relative sensing capabilities available on each spacecraft. The initial connection graph is given in Fig. 6(a), and the resulting MST is given in Fig. 6(b). A key point in this example is to highlight the non-triviality of the resulting topology.

Another component of the mission involves collecting data from an asteroid that requires the pico-satellite team to rendezvous with an asteroid. For this scenario, we first consider a rendezvous problem for each pico-satellite individually. Each satellite is assumed to have continuous actuation on each axis. We also introduce disturbances in the form of process noise for the actuators and measurement noise for the sensors. The noises are assumed to be white Gaussian with $\sigma_w^2 = 0.1$ for the process and $\sigma_v^2 = 0.01$ for the sensors. Contrary to the previous example, we will assume homogeneous agent dynamics generated by the Hill's equations which are used to describe the linearized relative dynamics of the agents with respect to the circular orbit, visualized in Fig. 7(a) [40]. The target asteroid is
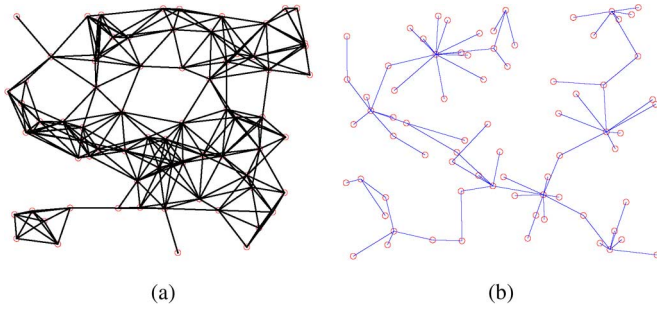
Fig. 6. Application example for Theorem 4.1: (a) random geometric graph with $r = 0.20$; (b) optimal spanning tree.
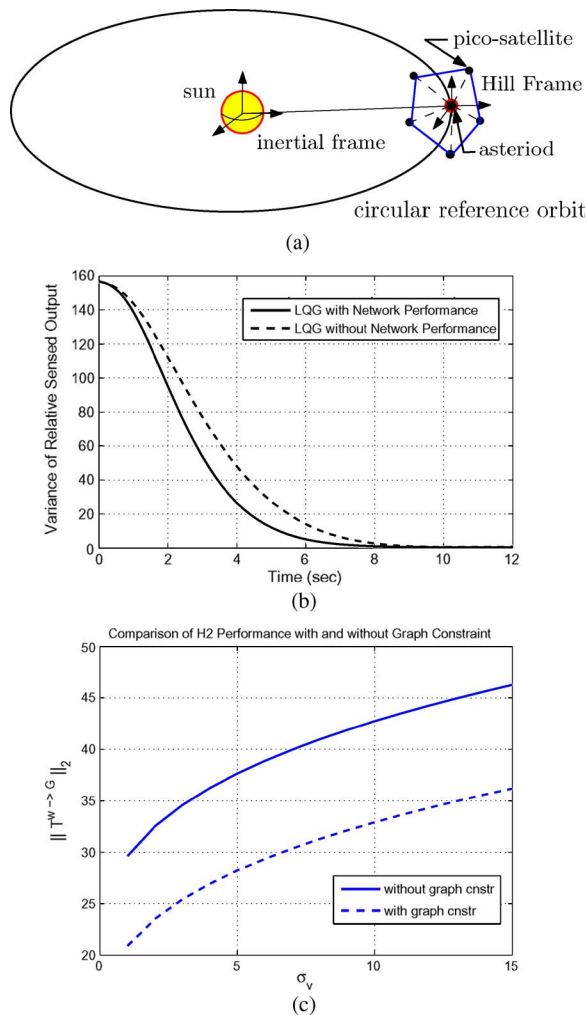

Fig. 7. (a) Hill frame for a circular orbit, (b) variance of $y_{\mathcal{G}}(t)$ for a system with RSN performance constraints (solid) and without (dashed), (c) performance of the system for increasing sensor noise with and without the RSN constraint.

assumed to be in a circular orbit around the Sun with radius of $r_o = 3 \times 10^9$ km. We next generate a random spanning tree graph and the results of Theorem 4.8 are applied to generate a control for each pico-satellite to drive them to the asteroid. We also address the issue in Remark 4.9 regarding the full-state information. For this example we employ LQG for estimation and control while including the additional performance constraint for the network. Fig. 7(b) depicts the variance of the RSN output $\mathbf{y}_{\mathcal{G}}(t)$ for the system using the network performance constraint

and the system without the constraint. This shows that the inclusion of the network performance constraint will tend to keep the agents closer together even in the presence of noise.

Remark 5.1: This example demonstrates that by including the network performance constraint in the objective, a greater sense of "team cohesiveness" can be achieved. This property is gained even without the active use of the relative measurements in the control. To further illustrate this point, Fig. 7(c) shows how the system norm $\|T_{hom}^{w \mapsto \mathcal{G}}\|_2$, changes as the noise on each satellite's sensor increases. In this figure, the solid line is the norm value for the system without the network performance constraint, while the dashed line includes this constraint, showing a better performance across all noise levels.

VI. CONCLUDING REMARKS

This paper focused on the development of graph theoretic performance bounds and synthesis techniques for distinct classes of relative sensing networks (RSN). The results of this paper highlight an important connection between certain graph-theoretic concepts and systems-theoretic properties. In particular, for the $\mathcal{H}_2$ performance, we find that spanning trees and the node degree of each agent are the defining features. In contrast, the $\mathcal{H}_\infty$ performance depends on the spectral norm of a node-weighted incidence matrix, a property dependent on the structure of the graph.

When minimizing an $\mathcal{H}_2$ performance objective for synthesis, it was shown that application of Kruskal's algorithm for finding the minimum weight spanning tree can be employed to design the optimal topology. Using methods from robust semidefinite programming, a synthesis procedure was then developed that aims to minimize the $\mathcal{H}_\infty$ performance of an RSN with uncertainty on the edge weights. For closing the inner-loop with $\mathcal{H}_2$ performance, an SDP approach was presented that had the feature of being separable across each agent. We also showed that with an appropriate choice of decentralized controllers, the well-studied consensus algorithm can be obtained, leading to a new interpretation of such systems.

This work also suggests that the relationship between systems-theoretic properties and graph properties in RSNs can be examined further in the systems and control community. In fact, we believe that developing efficient solution methods for the synthesis of such systems will involve further reinterpretations of results from graph theory and combinatorial optimization in the context of systems and control theory.

REFERENCES

[1] Autonomous Nanotechnology Swarm [Online]. Available: http://ants.gsfc.nasa.gov

[2] I. F. Akyildiz, Y. Sankarasubramaniam, and E. Cayirci, "A survey on sensor networks," *IEEE Commun. Mag.*, vol. 40, no. 8, pp. 102–114, Aug. 2002.

[3] B. Awerbuch, "Optimal distributed algorithms for minimum weight spanning tree, counting, leader election, and related problems," in *Proc. 19th Ann. ACM Conf. Theory of Computing—STOC '87*, New York, 1987, pp. 230–240, ACM Press.

[4] P. Barooah, N. Machado Da Silva, and J. P. Hespanha, *Distributed Optimal Estimation From Relative Measurements for Localization and Time Synchronization*. Berlin/Heidelberg: Springer-Verlag, 2006, vol. 4026, Lecture Notes in Computer Science, ch. 17, pp. 266–281.

[5] A. Behar, J. Matthews, F. Carsey, and J. Jones, "NASA/JPL tumbleweed polar rover," in *Proc. 2004 IEEE Aerospace Conf.*, 2004, pp. 388–395.

[6] A. Ben-Tal, L. El Ghaoui, and A. Nemirovski, *Robust Optimization*. Princeton: Princeton Univ. Press, 2009.

[7] G. Chen and Z. Duan, "Network synchronizability analysis: A graph-theoretic approach," *Chaos (Woodbury, N.Y.)*, vol. 18, no. 3, p. 037102, 2008.

[8] T. Corazzini, A. Robertson, J. C. Adams, A. Hassibi, and J. P. How, "GPS sensing for spacecraft formation flying," presented at the Institute of Navigation GPS-97 Conf., Kansas City, MO, Sep. 1997.

[9] "LISA: Laser Interferometer Space Antenna for the Detection and Observation of Gravitational Waves," LISA Project Internal Rep. No. LISA-PRJ-RP-0001, May 2009.

[10] G. E. Dullerud and F. Paganini, *A Course in Robust Control Theory: A Convex Approach*. New York: Springer-Verlag, 2000.

[11] J. A. Fax and R. M. Murray, "Information flow and cooperative control of vehicle formations," *IEEE Trans. Autom. Contr.*, vol. 49, no. 9, pp. 1465–1476, Sep. 2004.

[12] C. Fridlund, "Infrared space interferometry-the DARWIN mission," *Adv. Space Res.*, vol. 30, no. 9, pp. 2135–2145, 2002.

[13] R. G. Gallager, P. A. Humblet, and P. M. Spira, "A distributed algorithm for minimum-weight spanning trees," *ACM Trans. Programming Languages Syst.*, vol. 5, no. 1, pp. 66–77, 1983.

[14] C. D. Godsil and G. Royle, *Algebraic Graph Theory*. New York: Springer, 2001.

[15] I. Gutman, "The star is the tree with greatest greatest Laplacian eigenvalue," *Kragujevac J. Math.*, vol. 24, pp. 61–65, 2002.

[16] F. Y. Hadaegh and R. S. Smith, "Control of deep-space formation-flying spacecraft: Relative sensing and switched information," *J. Guidance, Contr., Dynamics*, vol. 28, no. 1, pp. 106–114, Jan. 2005.

[17] R. A. Horn and C. R. Johnson, *Matrix Analysis*. New York: Cambridge Univ. Press, 1991.

[18] R. A. Horn and C. R. Johnson, *Topics in Matrix Analysis*. New York: Cambridge Univ. Press, 1991.

[19] J. P. How, R. T. D. Weidowf, K. Hartmanf, and F. Bauer, "Orion: A low-cost demonstration of formation flying in space using GPS," in *Proc. Astrodynam. Specialist Conf.*, 1998, pp. 276–286.

[20] , C. R. Johnson, Ed., *Matrix Theory and Applications*. Phoenix, AZ: American Mathematical Society, 1990.

[21] T. Kailath, *Linear Systems*. Englewood Cliffs, NJ: Prentice Hall, 1980.

[22] U. Khan, S. Kar, and J. M. F. Moura, "Distributed sensor localization in random environments using minimal number of anchor nodes," *IEEE Trans. Signal Process.*, vol. 57, no. 5, pp. 2000–2016, May 2009.

[23] U. Khan and J. M. F. Moura, "Distributing the Kalman filter for large-scale systems," *IEEE Trans. Signal Process.*, vol. 56, no. 10, pp. 4919–4935, 2008.

[24] B. H. Korte and J. Vygen, *Combinatorial Optimization: Theory and Algorithms*. Berlin, Germany: Springer-Verlag, 2000.

[25] P. R. Lawson, "The Terrestrial Planet Finder," in *Proc. IEEE Aerospace Conf.*, 2001, pp. 2005–2111.

[26] Z. Li, Z. Duan, G. Chen, and L. Huang, "Consensus of multi-agent systems and synchronization of complex networks: A unified viewpoint," *IEEE Trans. Circuits Syst. I, Reg, Papers*, 57, no. 1, pp. 1–12, Jan. 2009.

[27] J. Löfberg, "Yalmip: A toolbox for modeling and optimization in MATLAB," in *Proc. CACSD Conf.*, Taipei, Taiwan, 2004, pp. 284–289.

[28] M. Mesbahi and F. Y. Hadaegh, "Formation flying control of multiple spacecraft via graphs, matrix inequalities, and switching," *AIAA J. Guidance, Contr., Dynam.*, vol. 24, no. 2, pp. 369–377, 2001.

[29] M. Mesbahi and M. Egerstedt, *Graph Theoretic Methods in Multiagent Networks*. Princeton, NJ: Princeton Univ. Press, 2010.

[30] R. Olfati-Saber, "Distributed Kalman filter with embedded consensus filters," in *Proc. 44th IEEE Conf. Decision Contr.*, 2005, pp. 8179–8184.

[31] R. Olfati-Saber, J. A. Fax, and R. M. Murray, "Consensus and cooperation in networked multi-agent systems," *Proc. IEEE*, vol. 95, no. 1, pp. 215–233, Jan. 2007.

[32] E. Olsenis, C. W. Park, and J. How, "3D Formation flight using differential carrier-phase GPS sensors," in *Proc. ION-GPS Conf.*, Nashville, TN, 1998, pp. 35–48.

[33] C. W. Park, P. Ferguson, N. Pohlman, and J. P. How, "Decentralized relative navigation for formation flying spacecraft using augmented CDGPS," in *Proc. Inst. Navigation GPS Conf.*, 2001, pp. 2304–2315.

[34] M. Petrovic and I. Gutman, "The path is the tree with smallest greatest Laplacian eigenvalue," *Kragujevac J. Math.*, vol. 24, pp. 67–70, 2002.

[35] G. Purcell, D. Kuang, S. Lichten, S. Wu, and L. Young, "Autonomous formation flyer (AFF) sensor technology development," in *21st Ann. AAS Guidance Contr. Conf.*, Breckenridge, CO, Jan. 1998, vol. 45.

[36] A. Rahmani, M. Ji, M. Mesbahi, and M. Egerstedt, "Controllability of multiagent systems from a graph-theoretic perspective," *SIAM J. Contr. Optimiz.*, vol. 48, no. 1, p. 162, 2008.

[37] J. Sandhu, M. Mesbahi, and T. Tsukamaki, "Relative sensing networks: Observability, estimation, and the control structure," in *IEEE Conf. Decision Contr.*, Dec. 2005, pp. 6400–6405.

[38] C. Scherer and P. Gahinet, "Multiobjective output-feedback control via LMI optimization," *IEEE Trans. Autom. Contr.*, vol. 42, no. 7, pp. 896–911, 1997.

[39] G. Sholomitsky, O. Prilutsky, and V. Rodin, "Infrared space interferometer," in *Int. Astronaut. Federation Congr.*, 1977.

[40] B. Wie, *Space Vehicle Dynamics and Control*. Reston, VA: American Institute of Aeronautics and Astronautics, Inc., 1998.

[41] D. Zelazo and M. Mesbahi, "On the observability properties of homogeneous and heterogeneous networked dynamic systems," *Proc. IEEE Conf. Decision Contr.*, pp. 2997–3002, Dec. 2008.

[42] D. Zelazo and M. Mesbahi, "Edge agreement: Graph-theoretic performance bounds and passivity analysis," *IEEE Trans. Autom. Contr.*, vol. 56, no. 3, pp. 544–555, Mar. 2011.

[43] D. Zelazo and M. Mesbahi, "Graph-theoretic methods for networked dynamic systems: Heterogeneity and $\mathcal{H}_2$ performance," in *Efficient Modeling and Control of Large-Scale Systems*, J. Mohammadpour and K. M. Grigoriadis, Eds. New York: Springer, 2010, pp. 219–249.

[44] F. Zhang, *Matrix Theory: Basic Results and Techniques*. New York: Springer-Verlag, 1999.

Daniel Zelazo was born in Milwaukee, WI, in 1977. He received the BSc. and M.Eng degrees in electrical engineering from the Massachusetts Institute of Technology, Cambridge, MA, in 1999 and 2001, respectively.

In 2009, he completed his Ph.D. from the University of Washington in Aeronautics and Astronautics. In between his Masters and Ph.D. degrees he worked at Texas Instruments, Japan, on audio compression algorithms. He is now a research associate at the University of Stuttgart, Germany, with research interests in networked dynamic systems, optimization, and graph theory.

Mehran Mesbahi received the Ph.D. degree from the University of Southern California, Los Angeles, in 1996.

He was a member of the Guidance, Navigation, and Analysis group at JPL from 1996–2000 and an Assistant Professor of Aerospace Engineering and Mechanics at University of Minnesota from 2000–2002. He is currently a Professor of Aeronautics and Astronautics at the University of Washington in Seattle. His research interests are distributed and networked aerospace systems, systems and control theory, and engineering applications of optimization and combinatorics.

Prof. Mesbahi was the recipient of NSF CAREER Award in 2001, NASA Space Act Award in 2004, UW Distinguished Teaching Award in 2005, and UW College of Engineering Innovator Award for Teaching in 2008.